http://dx.doi.org/10.5012/bkcs.2014.35.6.1737

Kinetically Controlled Growth of Gold Nanoplates and Nanorods *via* a One-Step Seed-Mediated Method

Soonchang Hong,[†] Jesus A. I. Acapulco Jr.,[†] Hee-Jeong Jang,[†] Akshay S. Kulkarni,[§] and Sungho Park[†,‡,*]

[†]*Department of Chemistry and* [‡]*Department of Energy Science, BK21 School of Chemical Materials Science, Sungkyunkwan University, Suwon 440-746, Korea.* [*]*E-mail: spark72@skku.edu*
[§]*Birla Institute of Technology and Sciences, Goa 403-726, India*
Received January 28, 2014, Accepted February 17, 2014

In this research, we further developed the one-step seed mediated method to synthesize gold nanoparticles (GNPs) and control their resulting shapes to obtain hexagonal, triangular, rod-shaped, and spherical gold nanostructures. Our method reveals that the reaction kinetics of formation of GNPs with different shapes can be controlled by the rate of addition of ascorbic acid, because this is the critical factor that dictates the energy barrier that needs to be overcome. This in turn affects the growth mechanism process, which involves the adsorption of growth species to gold nanoseeds. There were also observable trends in the dimensions of the GNPs according to different rates of addition of ascorbic acid. We performed further analyses to investigate and confirm the characteristics of the synthesized GNPs.

Key Words : Anisotropic, Isotropic, Gold nanoparticles, Growth kinetics, Seed mediated synthesis

Introduction

Metallic nanomaterials, either in pure form[1,2] or mixed with other compounds[3-5] and having different geometrical structure[6] possess unique optical, electronic, and catalytic properties. Among the various metallic nanomaterials, gold nanoparticles (GNPs) are widely applied in catalysis,[7] electronics,[8] and diagnostics.[9] Researchers have investigated variously shaped GNPs, especially anisotropic plate-shaped[10] and rod-shaped[11,12] GNPs. However, the mechanism of growth of these anisotropic GNPs is still not yet fully understood, so it remains challenging to synthesize complex GNPs of similar sizes that are homogenous in shape. Seed-mediated,[13,14] photochemical,[15] and biological[16] procedures are commonly used to synthesize GNPs.

Seed-mediated growth, which was pioneered by Natan *et al*.,[17] Murphy *et al.*,[18-20] and among others,[21] is the fundamental method used to control the dimensions of GNPs. This method has been used to synthesize gold nanoplates and nanorods. It involves using surfactants to form a template on which growth species assemble, resulting in variously shaped GNPs.[13,14] Usually, production of growth species are controlled by a mild reducing agent, such as ascorbic acid.[12,22,23]

Three-step seed-mediated synthesis is a method used to synthesize anisotropic GNPs in aqueous solution; it involves sequentially adding of aliquots one after another from three flasks containing different solutions. Murphy *et al*.[12] employed this procedure to obtain gold nanorods with an aspect ratio (length/width) greater than 10, while Mirkin *et al*.[10] extended this method to gold nanoplates and reported production of gold triangular nanoplates with an average width of 125 nm. Correct and careful use of hand techniques is critical when using the three-step seed-mediated method to successfully produce anisotropic GNPs.

An improved seed-mediated method in wet chemistry to synthesize anisotropic GNPs was then reported. This method uses silver ions to reduce the number of required synthesis steps from 3 to 1, and greatly increases the yield of gold nanorods (up to 90%) and has been widely adopted which is referred to as the one-step seed mediated method. However, this method produces GNPs with small dimensions. Gold nanorods with aspect ratios between 1 to 5 were reported by the Oddershede[24] and Murphy[25] research groups. In addition, Chung *et al.*[26] managed to produce gold nanoprisms with an edge length of 98 ± 17 nm, while Huang *et al.*[27] reported a one-step seed-mediated method (without silver ions) to synthesize hexagonal and triangular gold nanoplates, where the smaller nanoplates were mainly triangular in shape while the larger nanoplates exhibited hexagonal and truncated triangular nanostructures. Although the one-step seed-mediated method can be used to obtain high quality and homogenous gold nanorods and nanoplates, it is still a challenge to produce GNPs with higher dimensions that are of good quality using this method.

To fully control the purity, shape, and size of GNPs, formation kinetics should be understood. Nanosphere homogeneity and size can be controlled kinetically through controlling the rate of addition of precursor.[28] However, this is only true at some point, because as the nanoparticle's size increases, so does the deviation value. Most literature reports have focused on temperature variation to kinetically control the morphology of GNP during synthesis. Tsai and colleagues[29] showed that the synthesis of GNPs at elevated room temperatures was kinetically favored due to instability of the surfactant that served as a template, resulting in the production of icosahedral and plate-like gold nanostructures. Gao *et al.*[30] also applied the same approach; they were able to restrain

the self-nucleation of silver quasi-nanospheres by controlling the reaction kinetics through controlling the reaction temperature and the amount of seed; they obtained good homogeneity under these reaction conditions. However, reactions carried out at high temperature produced significant amounts of pseudo-spherical nanostructures, because temperature is directly proportional to surface diffusion, which affects the Oswald ripening process.

In this paper, we use the one-step seed mediated method, without silver ions at room temperature, to produce high aspect ratio (> 5) gold nanorods. We show that it is possible to specifically tune the size and shape of the gold nanoplates by controlling the reaction kinetics where concentrations, volumes, and temperature are held constant throughout this experiment while the rate of production of monomer was changed by controlling the rate of addition of ascorbic acid. The formation of thermodynamically favorable spheres appears to be unavoidable when synthesizing plate and rod-like gold nanostructures; preventing the production of gold nanospheres therefore still remains a challenge. We elucidate, for the first time, the kinetic principles underlying the formation of isotropic (spheres) and anisotropic GNPs (plates and rods). We also present the deduced reaction pathway to which the reaction would proceed depending upon the production rate of the monomers that illustrate the energy barrier and final energy differences between isotropic and anisotropic GNPs.

Experimental

Chemicals. Sodium iodide (NaI), ascorbic acid, and cetyltrimethylammonium bromide (CTAB) (Fluka) were purchased from Sigma-Aldrich. Gold chloride hydrate ($HAuCl_4 \cdot 3H_2O$) was purchased from KOJIMA. Sodium borohydride ($NaBH_4$) was purchased from JUNSEI. Ultra-pure water (18.2 $M\Omega cm^{-1}$) was used for all experiments.

Seed Preparation. GNP seeds with an average diameter of 5.2 ± 0.6 nm were prepared using the method reported by Millstone *et al.*[10] A solution containing 18 mL of ultra-pure water and 0.5 mL of 10 mM sodium citrate was used to reduce 0.5 mL of 10 mM $HAuCl_4$ with 0.5 mL of 100 mM $NaBH_4$ under vigorous stirring. Upon addition of $NaBH_4$, the solution turned a reddish orange color and was stirred for an additional minute. The resulting mixture was aged for 2-6 h to allow the hydrolysis of unreacted $NaBH_4$. To confirm the average diameter of GNPs, GNP seeds must exhibit a plasmon resonance peak at 500 nm.

Synthesis of Gold Nanoplates and Nanorods. Gold nanoplates were synthesized from 5.2 ± 0.6 nm gold nanoseeds by a one-step seed-mediated method with iodide ions. A 75 mL aliquot of 0.05 M aqueous CTAB solution, 37.5 μL of 0.01 M NaI, 1 mL of 20 mM aqueous $HAuCl_4 \cdot 3H_2O$ solution, and 40 mL of gold nanoseeds were mixed in a flask. A 30 mL of 0.01 M ascorbic acid was then added at different rates of addition: 0.5 mL/min, 1 mL/min, 2 mL/min, 3 mL/min, or all at once (abruptly added). Sodium iodide was added for the synthesis of plate-like gold nanostructures, while rod-like nanorods were synthesized in the absence of sodium iodide. Spherical gold nanostructures were obtained regardless of whether sodium iodide was present or not. Synthesized GNPs were obtained by precipitation for 4 hours after synthesis, while the mixture to which ascorbic acid was abruptly added was centrifuged at 9000 rpm for 10 minutes because no precipitate was observed (data not shown).

Instrumentation. A KD Scientific syringe pump was used to control the rate of addition of ascorbic acid. Synthesized GNPs were characterized using a JEM-2100F to obtain high-resolution transmission electron microscopy (HRTEM) images. A JEOL 7000F and JEOL 7600F were used to obtain Field emission scanning electron microscopy (FESEM) images and an Ultima IV Rigaku was used to obtain X-ray diffraction (XRD) patterns. UV-vis extinction spectra were acquired using S-3100 Scinco and UV-3600 Shimadzu spectrophotometers.

Results and Discussion

FESEM images of GNPs synthesized in the presence of iodide ions at various rates of addition of ascorbic acid (0.5 mL/min, 1 mL/min, 2 mL/min, 3 mL/min, and abrupt addition) are shown in Figures 1(a)-(e), respectively. The percent yield of gold nanoplates and spherical gold nanostructures was determined by counting nanostructures in the FESEM images; results are presented in Table 1. As the rate of addition of ascorbic acid increased from 0.5 to 2 mL/min to abrupt, the shapes of the resulting gold nanostructures changed from hexagonal plates to triangular plates to spherical GNPs, respectively, while addition rates of 1 and 3 mL/min showed the transition to produce the majority of synthesized GNPs. We used UV-vis extinction spectroscopy (Fig. 1(f)) to further confirm the homogeneity, shape, and size of the GNPs. We have previously reported the spectra behavior of gold hexagonal nanoplates and our results in Figures 1(a) and (b) are comparable to our previous findings; however, the nanoplates generated in the current study were larger,

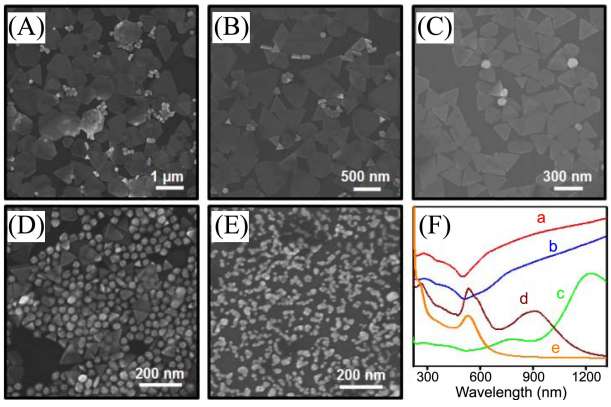

Figure 1. FESEM images of the synthesized gold nanostructures of plates and spheres with the presence of iodide ions at (A) 0.5 mL/min, (B) 1 mL/min, (C) 2 mL/min, (D) 3 mL/min, and (E) abrupt addition of ascorbic acid. (F) UV-vis extinction spectra a, b, c, d, and e for samples synthesized under conditions A, B, C, D, and E, respectively.

Table 1. Percent yield at varying addition rate of ascorbic acid in the presence of iodide ion

Gold nanostructures	Addition rate (mL/min)				
	0.5	1	2	3	Abrupt
Plates	54%	83%	94%	16%	0%
Spheres	46%	17%	6%	84%	100%

which may have resulted in unclear peaks. Among the spectra of all the samples, the samples obtained after adding ascorbic acid at 2 mL/min (spectra c) showed the most ideal spectra for gold triangular nanoplates based on the two observable peaks, which were assigned as dipole localized surface plasmon resonance (LSPR) mode located at the near-IR region (1234 nm) and inplane quadrupole LSPR mode at the visible region (784 nm), respectively, in accordance with our previous publications.[32-34] We assigned the two peaks observed in spectra d, from the acquired GNPs shown in Figure 1(d), to the LSPR mode mixture of nanospheres (538 nm) and nanoplates (923 nm), while the synthesized GNPs shown in Figure 1(e) (spectra e) only exhibited one peak (530 nm) corresponding to dipolar plasmon resonance of gold nanospheres.

Because precipitation was the only purification method that we used, we were able to compare the weights of the acquired GNPs. Images A, B, and D in Figure 1 show that the acquired GNPs (plates and spheres) had comparable weights. Given that larger GNPs contain more gold atoms than smaller GNPs, our results indicate that the acquired weight is inversely related to the rate of addition of ascorbic acid, as measured from the FESEM images. Image C clearly shows that there was a large difference in weight between the synthesized anisotropic GNPs (plates) and the by-product isotropic GNPs (spheres), resulting in good homogeneity of the desired product after precipitation.

Gold nanoplates are produced primarily due to the preferential adsorption of iodide ions on the (111) facet of gold nanoseeds, because the CTAB bilayer stabilizes the growth of gold nanoseeds, leading to a higher growth rate on the (110) facet than on the (111) facet.[26] We found that it was also possible to produce hexagonal gold nanoplates using the one-step seed-mediated method in contrast to our previous work,[31] where we employed shape transformation of GNPs from triangular to hexagonal gold nanoplates. Shape transformation occurred by selectively etching out the high surface area (vertex) of the triangular nanoplate followed by a ripening process, which yielded hexagonal gold nanoplates. In this study, we were able to directly produce hexagonal gold nanoplates through seed-mediated method by adding ascorbic acid at a low rate.

These findings can also be applied to the synthesis of other GNPs, despite differences in growth mechanism. For example, gold nanorods are synthesized in the absence of iodide ions, and growth involves a "zipping" formation mechanism.[6] We used our developed method to synthesize gold nanorods where we varied the rate of addition of ascorbic acid. We

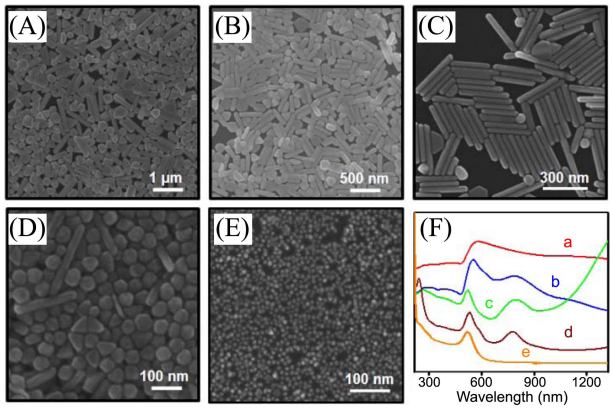

Figure 2. FESEM images of the synthesized rods and spheres gold nanostructures in the absence of iodide ion at (A) 1 mL/min, (B) 2 mL/min, (C) 3 mL/min, (D) 4 mL/min, and (E) abrupt addition of ascorbic acid. (F) UV-vis extinction spectra a, b, c, d, and e for samples synthesized under conditions A, B, C, D, and E, respectively.

Table 2. Percent yield at varying addition rate of ascorbic acid in the absence of iodide ion

Gold nanostructures	Addition rate (mL/min)				
	1	2	3	4	Abrupt
Rods	30%	61%	92%	8%	0%
Spheres	70%	39%	8%	92%	100%

observed similar trends to those we observed for the gold nanoplates, as shown in Figure 2 and Table 2. In particular, the dimensions of the synthesized gold nanorods decreased as the rate of addition of ascorbic acid increased (measured dimensions displayed in Table 3); addition of ascorbic acid at 3 mL/min yielded gold nanorods with an aspect ratio of 6, which was the highest aspect ratio measured among our synthesized gold nanorods. Furthermore, the spectra of gold nanostructures that formed when ascorbic acid was added at 3 mL/min (spectra c in Fig. 2(f)) showed the typical transverse and longitudinal modes of gold nanorod structures at 522 nm and beyond 1200 nm, respectively, while we assigned the peak at 793 nm to longitudinal quadruple surface plasmon resonance.[35] These results indicate that kinetic control during synthesis facilitates the growth of GNPs with various shapes.

The crystallinity of the synthesized plates and rods GNPs was confirmed by HRTEM images and XRD patterns (shown in Fig. 3). Both exhibited an ordered crystal lattice. Single crystalline structure of the synthesized gold nanoplates and nanorods was confirmed based on the well-resolved lattice fringe (Fig. 3(A)-(B)) with a spacing of 0.236 nm, which is close to the value we reported previously[31] that reflects the forbidden 1/3{422} reflection. Typical FFT patterns of the gold nanostructures of plates and rods were obtained by directing the incident electron beam perpendicular to the {111} facet of the synthesized GNPs. The XRD pattern (Fig. 3(C)) of the synthesized gold nanoplate showed {111} and

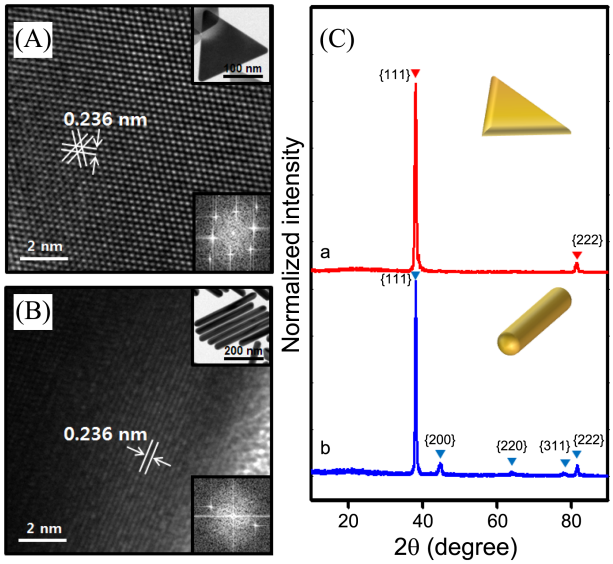

Figure 3. HRTEM images of (A) gold nanoplate, and (B) gold nanorod with TEM image and fast Fourier transform (FFT) pattern located at right upper and lower insets, respectively. (C) The X-ray diffraction (XRD) pattern of (a) plate, and (b) rod gold nanostructures.

{222} diffraction peaks, corresponding to angles of 38.06° and 81.46°, respectively, implying reflections of face-centered cubic (fcc) gold, while for gold nanorods, diffraction peaks were present at {111}, {200}, {220}, {311}, and {222}, consistent with previous studies.[36,37]

The rate of formation of monomer can be used to control the synthesis of nanoparticles.[38] Because size can influence optical properties,[39] we assigned different reaction rate constants based on the addition rate of ascorbic acid, as shown in Figure 4(A). The slowest addition of ascorbic acid, 0.5 mL/min (k_1) for gold nanoplates and 1 mL/min (k_1) for gold nanorods, resulted in the formation of anisotropic GNPs with the highest dimensions, while abrupt addition of ascorbic acid, denoted as k_6, yielded gold nanospheres. Proposed

Table 3. Summarized measured dimensions of the synthesized GNPs at varying addition rate of ascorbic acid

Addition rate of ascorbic acid (mL/min)	Dimension of synthesized anisotropic GNPs (nm)			
	Plate		Rod	
	Hexagonal	Triangular	Length	Width
0.5	651 ± 141	594 ± 241	–	–
1.0	258 ± 56	356 ± 158	666 ± 208	224 ± 31
2.0	161 ± 18	187 ± 22	289 ± 64	79 ± 8
3.0	73 ± 1	63 ± 19	272 ± 54	44 ± 5
4.0	–	–	132 ± 56	30 ± 13

reaction pathway will be discussed later. As commonly observed in other research studies, synthesis of anisotropic GNPs was accompanied by the formation of the by-product of gold nanospheres.[11,37,40] Therefore, these gold nanospheres are competitor GNPs and by plotting the diameter of the by-product as a function of the flow rate of ascorbic acid (Fig. 4(b)), we found that the size of the gold nanospheres was inversely proportional to the flow rate, and this relationship also applies to anisotropic GNPs (Table 3). However, as particle dimensions increase, so does the coefficient of variation, because a low rate of addition of ascorbic acid leads to a smaller concentration of monomer than the minimum concentration required for nucleation, resulting in suppression of the nucleation process and maximization of the growth process, which in turn leads to unequal nucleation distribution to every seed while further growth of randomly-produced gold nuclei is also occurring.

In contrast, abrupt addition of ascorbic acid resulted in the synthesis of gold nanospheres regardless of the presence or absence of iodide ions. According to Cao,[44] this can be explained by the rate of nucleation per unit volume and per unit time denoted as RN, as follows:

$$RN = \{C_o kT/(3\pi\lambda^3\eta)\}\exp(-\Delta G^*/kT) \quad (1)$$

where λ is the diameter of the growth species, η is the

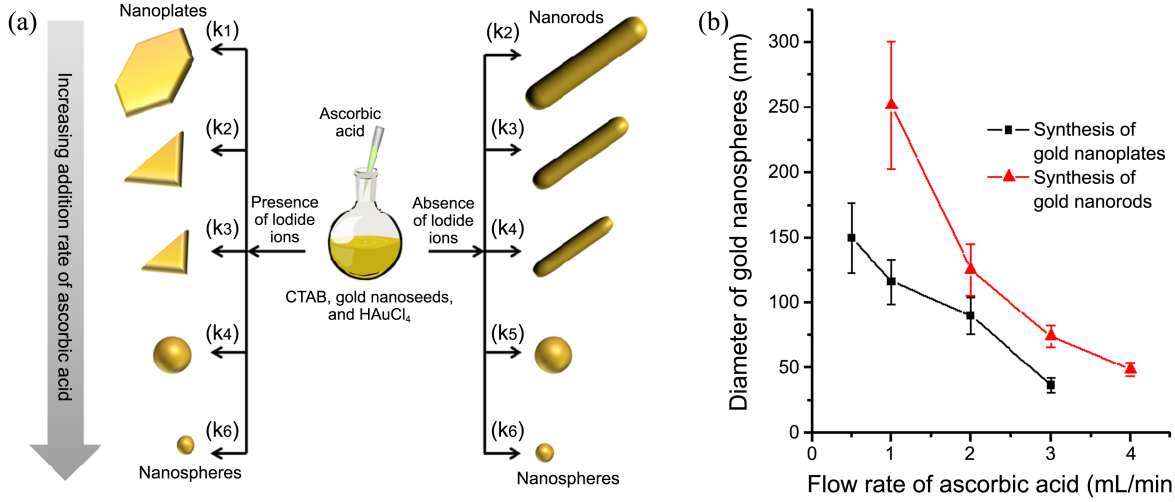

Figure 4. (a) Schematic diagram of the one-step method to synthesize GNPs showing the obtained result from different reaction rate, and (b) Plot of measured dimension versus flow rate of ascorbic acid with standard deviation.

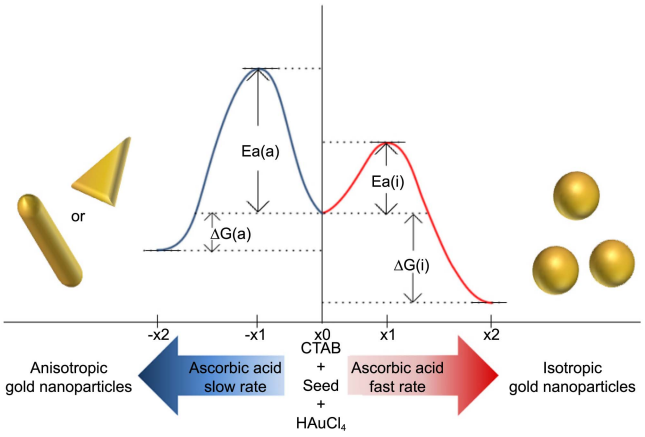

Scheme 1. Proposed schematic diagram of the reaction pathway during the synthesis of kinetically controlled GNPs.

viscosity of the solution, ΔG^* is the minimum energy to form a nuclei, k is the Boltzmann constant, and T is the temperature.

This indicates that a high initial concentration or supersaturation of ascorbic acid (large number of nucleation sites present), low viscosity, and a low critical energy barrier favor the formation of large numbers of nuclei. For a given concentration of solute, a larger number of nuclei means smaller-sized nuclei. The fastest addition rate (k_5) resulted in a high initial concentration of ascorbic acid, which in turn led to the production of small homogenous gold nanospheres from a large number of small nuclei during the nucleation process.

Formation of anisotropic (plate- and rod-like) or isotropic (spheres) GNPs can be explained by the Gibbs free energy of the system (y-axis in Scheme 1). The solution is at equilibrium state (stable Gibbs free energy) with all species in aqueous ionic state before the addition of ascorbic acid (point x0 in Scheme 1). In this state, the nitrogen of CTAB releases bromide to replace the proton of $HAuCl_4$.[41] For illustration purposes, we denote negative coordinates (left side) as anisotropic GNPs and positive coordinates (right side) as isotropic GNPs.

The CTA-$AuCl_4$ formed then serves as a precursor for GNP formation by reduction of Au(III) to Au(I) and finally to Au(0) by deprotonation of ascorbic acid.

Because the amount of ascorbic acid is greater than the amount of CTA-$AuCl_4$, CTA-$AuCl_4$ is the limiting reactant, resulting in complete reduction of Au(III) to Au(I). An excess amount of ascorbic acid will further reduce Au(I) to Au(0), favoring the formation of GNPs. However, the major factor that dictates the resulting shape of GNPs is the addition rate of ascorbic acid. As mentioned earlier, there are two directions that the reaction can proceed after the addition of ascorbic acid; to the right to produce gold nanospheres, or to the left to produce anisotropic GNPs. The reaction will proceed to the right at high reaction rates, while it will proceed to the left at low reaction rates. When ascorbic acid is added, the solution will exceed its equilibrium solubility; in other words, the solution is supersaturated and has high Gibbs free energy. The supersaturated solution will tend to reduce the overall Gibbs free energy of the system to acquire equilibrium (point –x2 or point x2) and to attain this, the solution will form a solid phase (colloids) in the form of GNPs. Ascorbic acid will be converted into dehydroascorbic acid, reducing the gold ions ($AuCl_2^-$ and $[Au(OH)_2]^-$) to metallic gold.[40,41] The formation of gold nanospheres is due to the lower energy barrier (point x1) required to form isotropic spheres than anisotropic GNPs (point –x1). Another factor that causes the formation of isotropic spheres is the nucleation process. Because synthesis of nanoparticles involves two processes, namely nucleation and growth, one must control the nucleation process to obtain pure non-spherical GNPs. Growth of GNPs then proceeds; however, the number of final particles is limited by the abstruse balance between the rates of nucleation and growth.[42,43] That is why seed-mediated growth is preferred. To decrease the probability of gold nanosphere formation, the concentration of the growth species must be less than the minimum concentration of nucleation so that nucleation process stops and growth process continues. Since the concentration of the growth species is highly dependent on ascorbic acid, decreasing the addition rate of ascorbic acid will reduce the concentration of the growth species compared to the minimum concentration for nucleation. In addition, we believe that the increase and decrease yield of anisotropic GNPs as the addition rate of ascorbic acid is increased are due to the atomic addition of gold on the seed. That is, at low and high addition rate of ascorbic acid, monomers are thermodynamically driven favoring the formation of nanospheres.

As stated above, we controlled the reaction rate by controlling the rate of addition of ascorbic acid. Hence, the activation energy for anisotropic GNPs, Ea(a), was greater than the activation energy for gold nanospheres, Ea(i), based on the reaction rate given by the Arrhenius equation.

Scheme 1 shows that the change in Gibbs free energy of anisotropic GNPs, ΔG(a), was lower than the change in Gibbs free energy of isotropic GNPs. This is because isotropic GNPs are thermodynamically favored, resulting in a low and stable energy profile compared to that of anisotropic GNPs.

Conclusion

In summary, we were able to control the homogeneity, shape, and size of gold nanoplates, nanorods, and nanospheres by controlling the rate of addition of ascorbic acid. By controlling this rate, we were able to control the kinetics of reaction for the formation of GNPs. We found that as the addition rate of ascorbic acid decreased, large dimension of GNPs were produced, regardless of the mechanism of formation. Moreover, abrupt addition of ascorbic acid favored the formation of gold nanospheres with small diameters regardless of whether iodide ions were present or absent. Our method offers a direct process to produce GNPs with large dimensions and to tune these dimensions for further applications. Lastly, we described the synthesis of GNPs in terms of energy as a function of the rate of addition of

ascorbic acid. The activation energy for the formation of anisotropic GNPs was higher than the activation energy for isotropic GNPs. Other parameters and conditions of the methodology presented here can be developed further to gain a better understanding of the mechanisms of formation of nanoparticles.

Acknowledgments. This work was supported by the National Research Foundation of Korea (National Leading Research Lab: 2012R1A2A1A03670370) and the Human Resources Development program (no. 20124010203270) of the Korea Institute of Energy Technology Evaluation and Planning (KETEP) grant funded by the Korea Government Ministry of Trade, Industry and Energy.

References

1. Xu, B. S.; Tanaka, S. I. *Scripta Mater.* **2001**, *44*(8-9), 2051-2054.
2. Yan, J. F.; Zou, G. S.; Wu, A. P.; Ren, J. L.; Yan, J. C.; Hu, A. M.; Zhou, Y. *Scripta Mater.* **2012**, *66*(8), 582-585.
3. Mahl, D.; Diendorf, J.; Ristig, S.; Greulich, C.; Li, Z. A.; Farle, M.; Koller, M.; Epple, M. *J. Nanopart. Res.* **2012**, *14*(10), 1153, 1-13.
4. Terzi, F.; Zanardi, C.; Daolio, S.; Fabrizio, M.; Seeber, R. *Electrochim. Acta* **2011**, *56*(10), 3673-3678.
5. Mott, D.; Luo, J.; Smith, A.; Njoki, P. N.; Wang, L. Y.; Zhong, C. J. *Nanoscale Res. Lett.* **2007**, *2*(1), 12-16.
6. Gao, J. X.; Bender, C. M.; Murphy, C. J. *Langmuir* **2003**, *19*(21), 9065-9070.
7. Thompson, D. T. *Nano Today* **2007**, *2*(4), 40-43.
8. Huang, D.; Liao, F.; Molesa, S.; Redinger, D.; Subramanian, V. *J. Electrochem. Soc.* **2003**, *150*(7), G412-G417.
9. Peng, G.; Tisch, U.; Adams, O.; Hakim, M.; Shehada, N.; Broza, Y. Y.; Billan, S.; Abdah-Bortnyak, R.; Kuten, A.; Haick, H. *Nat. Nanotechnol.* **2009**, *4*(10), 669-673.
10. Millstone, J. E.; Wei, W.; Jones, M. R.; Yoo, H. J.; Mirkin, C. A. *Nano Lett.* **2008**, *8*(8), 2526-2529.
11. Millstone, J. E.; Metraux, G. S.; Mirkin, C. A. *Adv. Funct. Mater.* **2006**, *16*(9), 1209-1214.
12. Gole, A.; Murphy, C. J. *Chem. Mater.* **2004**, *16*(19), 3633-3640.
13. Johnson, C. J.; Dujardin, E.; Davis, S. A.; Murphy, C. J.; Mann, S. *J. Mater. Chem.* **2002**, *12*(6), 1765-1770.
14. Sau, T. K.; Murphy, C. J. *J. Am. Chem. Soc.* **2004**, *126*(28), 8648-8649.
15. Kim, F.; Song, J. H.; Yang, P. D. *J. Am. Chem. Soc*. **2002**, *124*(48), 14316-14317.
16. Shankar, S. S.; Rai, A.; Ankamwar, B.; Singh, A.; Ahmad, A.; Sastry, M. *Nat. Mater.* **2004**, *3*(7), 482-488.
17. Brown, K. R.; Walter, D. G.; Natan, M. J. *Chem. Mater.* **2000**, *12*(2), 306-313.
18. Jana, N. R.; Gearheart, L.; Murphy, C. J. *Adv. Mater.* **2001**, *13*(18), 1389-1393.
19. Jana, N. R.; Gearheart, L.; Murphy, C. J. *J. Phys. Chem. B* **2001**, *105*(19), 4065-4067.
20. Jana, N. R.; Gearheart, L.; Murphy, C. J. *Langmuir* **2001**, *17*(22), 6782-6786.
21. Lohse, S. E.; Murphy, C. J. *Chem. Mater.* **2013**, *25*(8), 1250-1261.
22. Goia, D. V.; Matijevic, E. *Colloids and Surfaces A* **1999**, *146*(1-3), 139-152.
23. Kim, F.; Sohn, K.; Wu, J. S.; Huang, J. X. *J. Am. Chem. Soc.* **2008**, *130*(44), 14442-14443.
24. Selhuber-Unkel, C.; Zins, I.; Schubert, O.; Sonnichsen, C.; *Nano Lett.* **2008**, *8*(9), 2998-3003.
25. Gou, L. F.; Murphy, C. J. *Chem. Mater.* **2005**, *17*(14), 3668-3672.
26. Ha, T. H.; Koo, H. J.; Chung, B. H. *J. Phys. Chem. C* **2007**, *111*(3), 1123-1130.
27. Chu, H. C.; Kuo, C. H.; Huang, M. H. *Inorg. Chem.* **2006**, *45*(2), 808-813.
28. Schwartzberg, A. M.; Olson, T. Y.; Talley, C. E.; Zhang, J. Z. *J. Phys. Chem. B* **2006**, *110*(40), 19935-19944.
29. Min-Chen, H.; Liu, R. S.; Tsai, D. P. *Cryst. Growth Des.* **2009**, *9*(5), 2079-2087.
30. Liu, X. X.; Yin, Y. D.; Gao, C. B. *Langmuir* **2013**, *29*(33), 10559-10565.
31. Hong, S.; Shuford, K. L.; Park, S. *Chem. Mater.* **2011**, *23*(8), 2011-2013.
32. Baik, H. J.; Hong, S.; Park, S. *J. Colloid Interf. Sci.* **2011**, *358*(2), 317-322.
33. Hong, S.; Choi, Y.; Park, S. *Chem. Mater.* **2011**, *23*(24), 5375-5378.
34. Kim, J.; Hong, S.; Jang, H. J.; Choi, Y.; Park, S. *J. Colloid Interf. Sci.* **2013**, *389*, 71-76.
35. Hong, S.; Shuford, K. L.; Park, S. *Chem-Asian J.* **2013**, *8*(6), 1259-1264.
36. Sun, J. H.; Guan, M. Y.; Shang, T. M.; Gao, C. L.; Xu, Z. *Sci. China Chem.* **2010**, *53*(9), 2033-2038.
37. Guo, Z. R.; Zhang, Y.; DuanMu, Y.; Xu, L.; Xie, S. L.; Gu, N. *Colloid Surface A* **2006**, *278*(1-3), 33-38.
38. Abecassis, B.; Testard, F.; Kong, Q. Y.; Francois, B.; Spalla, O. *Langmuir* **2010**, *26*(17), 13847-13854.
39. Nikoobakht, B.; El-Sayed, M. A. *Chem. Mater.* **2003**, *15*(10), 1957-1962.
40. Wu, H. Y.; Liu, M.; Huang, M. H. *J. Phys. Chem. B* **2006**, *110*(39), 19291-19294.
41. Khan, Z.; Singh, T.; Hussain, J. I.; Hashmi, A. A. *Colloid Surface B* **2013**, *104*, 11-17.
42. van Embden, J.; Sader, J. E.; Davidson, M.; Mulvaney, P. *J. Phys. Chem. C* **2009**, *113*(37), 16342-16355.
43. Shevchenko, E. V.; Talapin, D. V.; Schnablegger, H.; Kornowski, A.; Festin, O.; Svedlindh, P.; Haase, M.; Weller, H. *J. Am. Chem. Soc.* **2003**, *125*(30), 9090-9101.
44. Cao, G. *Nanostructures & Nanomaterials; Synthesis, Properties & Applications*; Imperial College Press: 2004; p 56.